

Single-mode transfective liquid crystal display tailored for wide-band single gamma curve

Jin Seog Gwag¹, You-Jin Lee², Jae-Hoon Kim^{1,2*}, Hyeok Jin Lee³, and Mi Hie Yi⁴

¹Research Institute of Information Display, Hanyang University, Seoul 133-791, Korea

²Department of Information Display, Hanyang University, Seoul 133-791, Korea

³Samsung Electronics, LCD R&D Center, Yongin-city, Gyeonggi-do, Korea

⁴Polymeric Nanomaterials Laboratory, Korea Research Institute of Chemical Technology, 100 Jang-dong, Yuseong, Daejeon 305-610, Korea

jhoon@hanyang.ac.kr

Abstract: This paper proposes a single cell gap transfective patterned vertically aligned liquid crystal mode with the same gamma curve for both reflective and transmissive operation. The gamma curve of the proposed transfective mode is obtained by tuning the chevron-type electrode structure in the reflective part to diminish the difference of the optical polarization path on the Poincare sphere, between the transmissive and reflective parts. Wide-band characteristics can be obtained by using in-cell $\lambda/4$ retardation films with different optic axes in the transmissive and reflective parts.

© 2008 Optical Society of America

OCIS codes: (230.0230) Optical devices; (230.3720) Liquid-crystal devices

References

1. M. Oh-e and K. Kondo, "Electro-optical characteristics and switching behavior of the in-plane switching mode," *Appl. Phys. Lett.* **67**, 3895-3897 (1995).
2. S. H. Lee, S. L. Lee, and H. Y. Kim, "Electro-optic characteristics and switching principle of a nematic liquid crystal cell controlled by fringe-field switching," *Appl. Phys. Lett.* **73**, 2881-2883 (1998).
3. T. Miyashita, Y. Yamaguchi, and T. Uchida, "Wide-Viewing-Angle Display Mode Using Bend-Alignment Liquid Crystal Cell," *J. Appl. Phys.* **34**, L177-L179 (1995).
4. J. S. Gwag, K.-H. Park, J. L. Lee, J. C. Kim, and T.-H. Yoon, "Two-Domain Hybrid-Aligned Nematic Cell Fabricated by Ion Beam Treatment of Vertical Alignment Layer," *Jpn. J. Appl. Phys.* **44**, 1875-1878 (2005).
5. J. S. Gwag, J. Fukuda, M. Yoneya, and H. Yokoyama, "In-plane bistable nematic liquid crystal devices based on nanoimprinted surface relief," *Appl. Phys. Lett.* **91**, 073504 (2007).
6. J. S. Gwag, Y.-J. Lee, M.-E. Kim, J.-H. Kim, J. C. Kim, and T.-H. Yoon, "Viewing angle control mode using nematic bistability," *Opt. Express*. **16**, 2663-2668 (2008).
7. H. Y. Kim, Z. Ze, S.-T. Wu, and S. H. Lee, "Wide-view transfective liquid crystal display for mobile applications," *Appl. Phys. Lett.* **91**, 231108 (2007).
8. S. H. Lee, K.-H. Park, J. S. Gwag, T.-H. Yoon, and J. C. Kim, "A Mutimode-Type Transfective Liquid Crystal Display Using the Hybrid-Aligned Nematic and Parallel Rubbed Vertically Aligned Modes," *Jpn. J. Appl. Phys.* **42**, 5127-5132 (2003).
9. J. S. Gwag, J. Park, Y.-J. Lee, and J.-H. Kim, "Electro-optical characteristics of reflective liquid crystal mode using π -cell for low power operation," *Appl. Phys. Lett.* **93**, 121103 (2008).
10. Y. J. Lim, J. H. Song, and S. H. Lee, "Transfective Liquid Crystal Display with Single Cell Gap and Single Gamma Curve," *Jpn. J. Appl. Phys.* **44**, 3080-3081 (2005).
11. Z. Ze, X. Zhu, R. Lu, T. X. Wu, and S. T. Wu, "Transfective liquid crystal display using commonly biased reflectors," *Appl. Phys. Lett.* **90**, 221111 (2007).
12. J. H. Hong, Y. J. Lim, M.-H. Lee, S. H. Lee, and S. T. Wu, "Electro-optic characteristics and switching principle of a single-cell-gap transfective liquid-crystal display associated with in-plane rotation of liquid crystal driven by a fringe-field," *Appl. Phys. Lett.* **87**, 011108 (2005).
13. Y.-J. Lee, T.-H. Lee, J.-W. Jung, H.-R. Kim, Y. Choi, S.-G. Kang, Y.-C. Yang, S. Shin, and J. H. Hoon, "Transfective Liquid Crystal Display with Single Cell Gap in Patterned Vertically Aligned Mode," *Jpn. J. Appl. Phys.* **45**, 7827-7830 (2006).
14. Y.-J. Lee, S.-G. Kang, T.-H. Lee, Y. Choi, H.-R. Kim, and J. H. Hoon, "Wide Viewing Transfective Liquid Crystal Display with a Patterned Electrode," *Mol. Cryst. Liq. Cryst.* **476**, 213-225 (2007).
15. K. Fujimori, Y. Narutaki, Y. Itoh, N. Kimura, S. Mizushima, Y. Ishii, and M. Hijikigawa, "New Color Filter Structure for Transfective TFT-LCD," *Digest of Technical Papers of 2002 Society for Information Display International Symposium* (Society for information Display, Boston, U. S. A., 2002), 1382-1385.
16. C.-J. Yu, D.-W. Kim, and S.-D. Lee, "Mutimode transfective liquid crystal display with a single cell

1. Introduction

Small liquid crystal displays (LCDs) have been developed for multimedia portable electronic devices such as mobile device applications, digital cameras, and personal digital assistants. Conventional portable devices have mainly used the transmissive LCDs, which shows excellent color images in indoor environments [1-6]. However, transmissive LCDs are not suitable for outdoor environments, especially under bright sunlight conditions. To enhance the readability for both indoor and outdoor use applications, transmissive LCDs, in which the transmissive and reflective parts are placed on the same pixel, have been extensively developed due to their portability, high visibilities and low power consumption [7-11]. However, due to the optical path difference between the transmissive and reflective regions, it is very difficult to match the electro-optical (EO) properties in both regions. The EO properties of an LCD are governed by the phase retardation of the incident polarized light, $R = \Delta n_{eff}d$, where Δn_{eff} , and d are the effective birefringence of the LC and cell gap, respectively. In general, in order to use the same LC mode in the two parts of transmissive LCDs, the cell gap in the transmissive part should be double that of the reflective part to match retardation. However, the manufacturing process to produce multi-cell gaps is cumbersome, and the optical properties are not good enough because of the misalignment of the LCs on the boundaries between different cell gaps. Moreover, the response times in both regions are different due to the cell gap difference. On the other hand, transmissive LCDs with a single cell gap (i.e., the same d in both parts) must use different modes, or different operating voltages, in the transmissive and reflective parts for the different Δn_{eff} in both parts. With this method, one cannot easily obtain single gamma characteristics due to the different electro-optic characteristics of the two modes. Therefore, it requires complex driving circuits to adjust the electro-optic characteristics of the two modes by independent control of the LC director in each mode [12]. In our previous research, we proposed single cell gap transmissive LCD mode for single gamma [13, 14]. However it is optimized for single wavelength (green), which cannot be applied to real color LCD applications due to the optical dispersion of LCs.

In this paper, a new wide band transmissive LCD mode is presented, with a single-cell gap using a single mode of a patterned vertically aligned (PVA) LC without the mismatch of the gamma curve and the response times. The electrode structures in the transmissive and reflective parts are tuned to adjust the optical paths between the two parts, and wide-band characteristics are realized by adopting an in-cell retardation film.

2. Optical design and experimental preparation

Fig. 1 shows the schematic diagram of the proposed transmissive LCD structure, which is composed of two crossed polarizers, a $\lambda/2$ film, two $\lambda/4$ films, and a vertical aligned LC layer where λ , the wavelength of the light, is set at 560 nm. To match the EO properties, the electrode was patterned with different angles, and used in-cell retardation films with different optic axes in the transmissive and reflective parts.

To determine the optic axes of the retardation films and the LC layer of this proposed mode, Stokes parameters were used. The Jones matrix of a phase retardation film can be expressed as

$$J_{film} = \begin{bmatrix} e^{i\frac{\pi d}{\lambda}n_e} & 0 \\ 0 & e^{i\frac{\pi d}{\lambda}n_o} \end{bmatrix}.$$

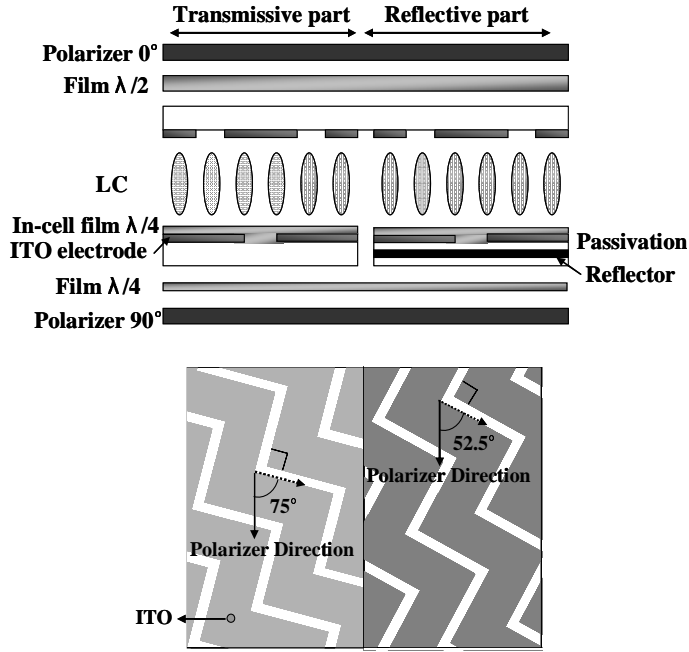


Fig. 1. (a) Schematic diagram of a cross-sectional view of the proposed PVA transfective LCD. (b) Patterned electrode structures in the transmissive and reflective parts.

Here, n_o is ordinary refractive index of film and n_e' is effective extraordinary refractive index expressed as

$$n_e' = \frac{n_e}{\sqrt{1 + ((n_e/n_o)^2 - 1) \sin^2 \theta}},$$

where θ is tilt angle of LC. To find the optic axes of the retardation films for good darkness in homeotropic LC alignment in the reflective part without an electric field, we calculate an optical polarization state of the light at reflector as follows:

$$\begin{bmatrix} E_x \\ E_y \end{bmatrix} = \begin{bmatrix} \cos \alpha_2 & -\sin \alpha_2 \\ \sin \alpha_2 & \cos \alpha_2 \end{bmatrix} J_{\lambda/4, film} \begin{bmatrix} \cos \alpha_2 & \sin \alpha_2 \\ -\sin \alpha_2 & \cos \alpha_2 \end{bmatrix} \begin{bmatrix} \cos \alpha_1 & -\sin \alpha_1 \\ \sin \alpha_1 & \cos \alpha_1 \end{bmatrix} \\ \times J_{\lambda/2, film} \begin{bmatrix} \cos \alpha_1 & \sin \alpha_1 \\ -\sin \alpha_1 & \cos \alpha_1 \end{bmatrix} \begin{bmatrix} 1 \\ 0 \end{bmatrix}$$

Here, α_1 and α_2 are the angles between the optic axis of the $\lambda/2$ and $\lambda/4$ retardation films and the optic axis of the top polarizer, respectively. In this calculation for a dark state, the light at the reflector must be a circular polarization to obtain 90° rotated linearly polarized light at final result before the polarizer. Therefore, in terms of Stokes parameters, $S_1 = S_2 = 0$ and $S_3 = 1$. In this case, $(\alpha_1 - 2\alpha_2) = \pm\pi/4$ and $\sin 2\alpha_1 = \pm 1/2$ are the conditions necessary to achieve the dark state with small dispersion. Therefore, $\alpha_1 = \pm 15^\circ$ and $\alpha_2 = \pm 75^\circ$. In the next step to achieve maximum reflectance, we determine the azimuthal

directions of the LCs falling by an electric field. In the above film conditions, when the directions are 52.5° , 142.5° , 232.5° , and 322.5° , maximum reflectance is obtained.

In order to make four LC domains, chevron-shaped ITO electrodes were used with different patterning angles in the transmissive and reflective parts, based on the results of the numerical calculations. The patterning angles of electrode were 75° and 165° at the transmissive part and 52.5° and 142.5° at the reflective part. The electrode width and gap (slit width) were periodically $70\ \mu\text{m}$ and $10\ \mu\text{m}$, respectively. In the first step of the photo-alignment, linearly polarized ultraviolet light (LPUV) with one polarization direction is illuminated to both the transmissive and reflective parts in the front side. In the next step, LPUV with a different polarization direction is illuminated to both parts in the back side. In this step, only a photo-alignment layer in the transmissive part is exposed to LPUV due to the self-mask effect of the reflector in the reflective part [15, 16]. Consequently, the optic axes of the transmissive and reflective parts are determined by the second and first LPUV exposure, respectively. Photo-alignment material (H-PSPI, KRICT I&E PRC) was used to produce the alignment of the in-cell retardation film. The easy axes of the alignment layer are 75° for the reflective part and 105° for the transmissive part, with respect to the top polarizer. The in-cell retardation film is made of a polymerisable nematic mixture (PNM, RMS-03-001C, Merck) with $n_o=1.529$ and $n_e=1.684$. In order to produce a thickness of $0.94\ \mu\text{m}$ corresponding to the retardation value of $\lambda/4$, the PNM dissolved in Propylene Glycol Monomethyl Ether Acetate (PGMEA) was coated on the photo-alignment layer at 6,000 rpm. It was dried at 60°C for 5 min and exposed to 365 nm UV light at 7.4 mW under a nitrogen environment for 30 min. AL1H659 (JSR CO., Japan) was used as the LC alignment material to align the LCs in the vertical direction in the initial state. Nematic LC MLC-6610 (Merck) was used with negative dielectric anisotropy, and the cell gap was maintained by $3.5\text{-}\mu\text{m}$ glass spacers. The LC injection was carried out at room temperature.

3. Simulation and experimental results

Figure 2 (a) shows the simulated and experimental results of the optical dispersion for dark and bright states in the reflective part, and the polarization path representation on a Poincare sphere, to describe the simple optical principle. As expected, very good dispersion in both dark and bright states was exhibited, even though there is some mismatch between the simulations and experimental behavior in the red and blue regions. The polarization paths for the reflective mode are described as a representation of the proposed transmissive mode. In the case of the dark state under field-off in the reflective mode, the linear polarized light to 0° direction by the input polarizer becomes linearly polarized light rotated by 30° as shown in path ① after passing through a $\lambda/2$ retardation film with an optic axis of 15° . Then, if the film is fitted in the green wavelength, blue and red wavelengths deviate from 30° -linear polarization. When the light passes through the LC layer, there is no change of polarization because liquid crystal molecules are aligned homeotropically. In the reflector, after passing the $\lambda/4$ in-cell retardation film with 75° -optic axis, all wavelengths meet on the north pole of the Poincare sphere, which means the left-handed circular polarization, as shown in path ②. The light reflected by the reflector is 120° -linear polarization after passing the $\lambda/4$ in-cell retardation film, but blue and red wavelengths are dispersed from 120° -linear polarization as shown in path ③. However, finally, all the wavelengths passing the $\lambda/2$ retardation film with an optic axis of 15° become 90° -linear polarization, as shown in path ④, which shows the dark state. Consequently, the dark state of the reflective mode exhibits optically wide-band characteristics. In the case of the white state under field-on in the reflective mode, the 30° -linearly polarized light passing through a $\lambda/2$ retardation film with an optic axis of 15° becomes 75° -linearly polarized light after passing through the LC layer with an optic axis of 52.5° as shown in path ②. When passing the $\lambda/4$ in-cell retardation film twice by the reflector, the 75° -linear polarization is not changed because the optic axis of the $\lambda/4$ in-cell retardation film is 75° . After passing the LC layer again, it becomes 30° linearly polarized light as shown in path ③. Finally, the light returns to the 0° -linear polarization state by the $\lambda/2$ retardation film as shown in path ④. Consequently, a proper white state is

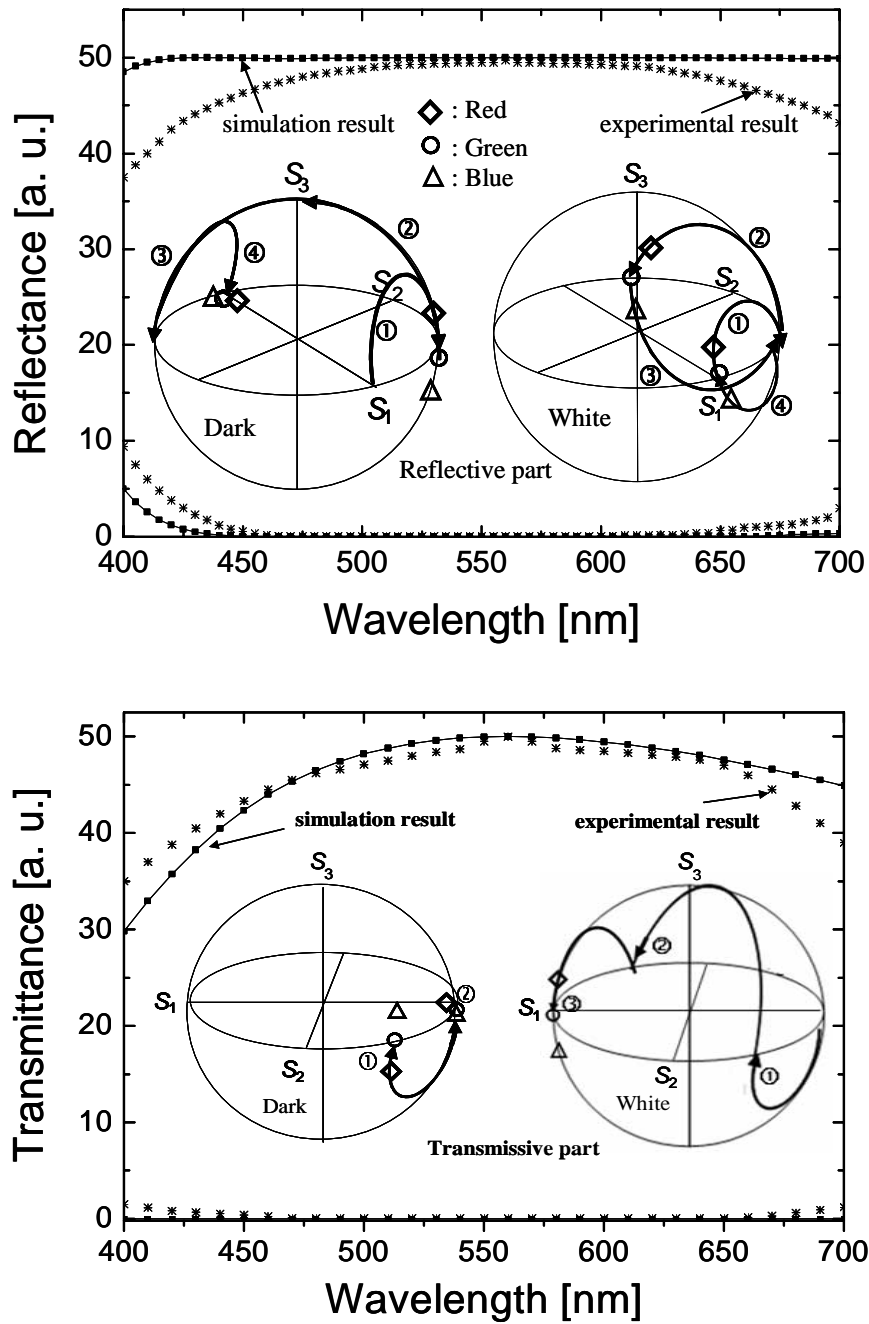


Fig. 2. Simulated and experimental optical dispersion characteristics of the proposed PVA transfective LCD. The results of the dark and bright states in the (a) reflective and (b) transmissive parts are shown. The inset is the polarization path representation on the Poincaré sphere, which describes the simple optical principle. ①, ②, ③, and ④ represent the polarization paths of the light when the light passes through each optical component in order.

obtained. The same description can be applied to the polarization paths of the dark and white states in the transmissive mode.

Under these fixed optical conditions of the reflective part, it is beneficial to find optical conditions of the transmissive part. For the dark state, in- and out-cell $\lambda/4$ retardation films have the same optic axis of 105° with respect to the optic axis of the top polarizer for compensating the $\lambda/2$ retardation film with an optic axis of 15° . For the bright state, the falling directions of LCs are also determined by an electric field to obtain maximum transmittance. As a result, when the optic axes of the LC layer are 75° , 165° , 255° , and 345° with respect to the top polarizer, maximum transmittance can be achieved. Under these conditions, the transmissive part shows good optical dispersion, as shown in Fig. 2 (b). This is also confirmed by the polarization path representation on a Poincare sphere for the dark and bright states of the transmissive part.

To confirm the theoretical study, samples were prepared with different electrode structures. First of all, the patterning angle was fixed at 75° in the transmissive part and the angles were changed to 52.5° , 50° , and 48° in the reflective part. As shown in Fig. 3, a single gamma curve could be obtained at the electrode structure of 48° , even though a slight reduction of reflectance occurs. This gamma matching is resulted from a modulated optic axis of the LC layer, which leads to the changed polarization path of the incident light on the Poincare sphere, which decreases the rate of increase of reflectance per unit voltage.

In addition, the chevron structure that is optimized at 48° did not degrade the optical dispersion characteristics. Fig. 4 shows numerically calculated isocontrast contours of the reflective and transmissive parts with the A-plate and negative C-plate as compensation films. Viewing angles over 52° and 58° in all directions of the reflective and transmissive parts, respectively, satisfy the contrast ratio limitation of 10:1. Based on these electro-optical characteristics, the proposed PVA transfective mode is sufficient for mobile applications.

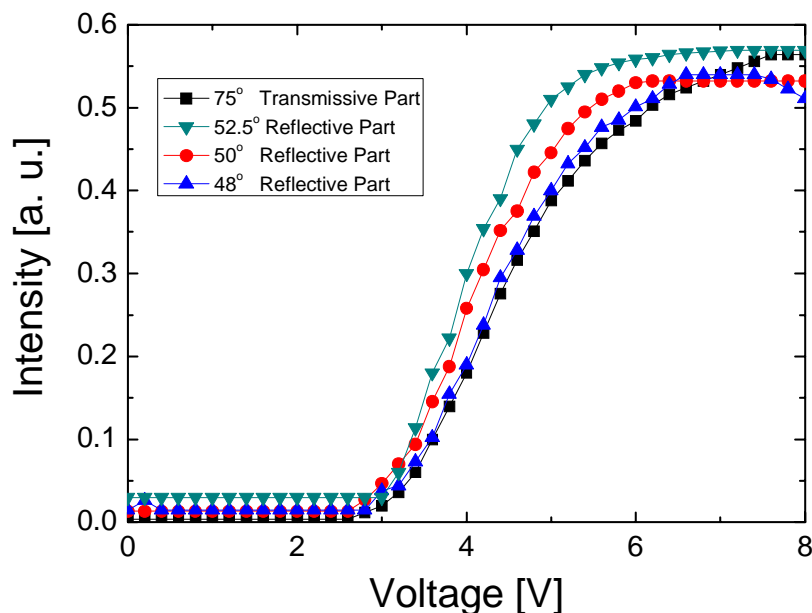


Fig. 3. Electro-optic characteristics with different patterning angles in the reflective part. The orientations of the chevron-type electrode in the reflective part are 52.5° , 50° , and 48° with respect to the top polarizer. The angle is fixed at 75° in the transmissive part.

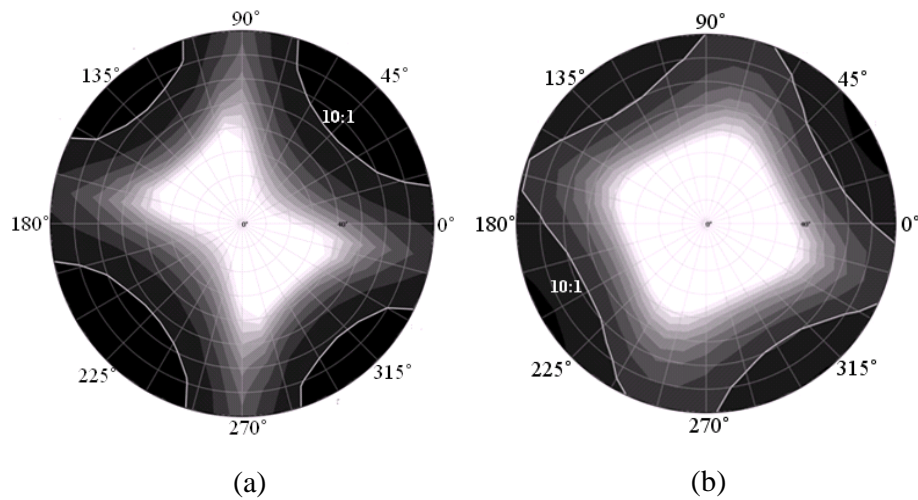


Fig. 4. Calculated viewing angle characteristics of the PVA transfective LCD with compensation films (A-plate and negative C-plate) in the (a) reflective part and in the (b) transmissive part.

4. Conclusion

A single-cell gap transfective PVA LCD for single gamma characteristics has been proposed. The optical polarization path difference between the transmissive and reflective parts is compensated by modulating the orientation of the chevron-shaped electrode and the wide-band characteristics are realized by adopting an in-cell retardation film made of photo curable PNM.

Acknowledgments

This work was supported by Samsung Electronics Co. Ltd. and the Korea Research Foundation Grant funded by the Korean Government (MOEHRD) (KRF-2006-005-J04103).